Investigation of Structural Damping Combining Linear and Non-linear Constrained Viscoelastic Mechanisms

Joseph M Ting
Massachusetts Institute of Technology
37-384
77 Massachusetts Ave.
Cambridge, MA 02139
(617) 253-7010

Connie K. Kim
Rocketdyne
Mail Code LB25
6633 Canoga Ave.
Canoga Park, CA 91303
(818) 700-4106

Prof. E.F. Crawley
Massachusetts Institute of Technology
37-341
77 Massachusetts Ave.
Cambridge, MA 02139
(617) 253-7510

Abstract

A damping scheme combining the linear effects of a viscoelastic material and the non-linear effects of an array of constraining plates was investigated. The damping material, Poron, was applied to the surface of an aluminum beam and constrained by a layer of thin aluminum segments. The segments were spaced so theat their edges would come into contact as the beam deflected. At deflections smaller than those which cause segment contact, the linear viscoelastic damping of the Poron was observed. At larger amplitudes, additional dissipation was expected due to the impact of the segments. Several configurations of the beams were tested in free fall in the ASTROVAC, a vacuum facility devoted to the testing of space structures. Compared to theory, the results of the linearly damped beams showed good correlation. The beams with contacting segments showed only a small amount of additional dissipation

1. Introduction

There are many ways that damping can be added to a structure. The method that will be discussed in this paper involves the use of a passive damping layer applied to the surface of a structure. Unconstrained viscoelastic damping materials usually produce small increases in linear damping. One way to increase damping is to add a layer of stiffer material to constrain the viscoelastic layer (Ungar , 1966, Kerwin, 1959). The constraining layer causes the viscoelastic material to shear, introducing additional energy loss. Because most of the shearing occurs at the ends of a constrained viscoelastic layer, damping can be increased by segmenting the constraining layer up so that there is more shear. In fact, the length of the constraints can be optimized (Plunkett and Lee, 1970).

Further increases of damping might be achieved by exploiting non-linear effects. In this project, an attempt was made to introduce non-linearities using the segmented constraint layer of an existing damping scheme. A viscoelastic layer was applied to the surface of several beams. This layer was then covered with a layer of constraining plates. The plates were spaced so that when the beam vibration exceeded a certain amplitude, the constraints would impact. The objective was to give large, non-linear damping at high amplitudes and smaller linear decay at low amplitudes.

2. Theoretical Background

The damping of a free viscoelastic layer applied to a beam in bending is due to losses through the stretching and bending of the layer (see Fig. 2.1). The associated loss factor (equal to twice the damping ratio ζ for light damping) for a beam treated on one side is given by,

$$\eta = \frac{\beta_2}{1 + \dfrac{k^2(1+\beta_2^2) + (r_1/H_{12})^2[(1+k)^2 + (\beta_2 k)^2]}{k[1 + (r_2/H_{12})^2[(1+k)^2 + (\beta_2 k)^2]]}} \tag{1}$$

where,

- β_2=Loss factor of viscoelastic layer
- $k=E_1H_1/E_2H_2$=Ratio of extensional stiffnesses
- $r_1=H_1/\sqrt{12}$=Radius of gyration of the beam
- $r_2=H_2/\sqrt{12}$=Radius of gyration of the viscoelastic layer
- $H_{12}=(H_1+H_2)/2$=Distance between neutral planes of the two layers
- E_i=Modulus of elasticity of the ith layer
- H_i=Thickness of ith layer

assuming a loss-less beam (Ungar, 1966). This loss factor is clearly related to the material and geometrical properties of the beam and viscoelastic layer. Adding this prediction to the material damping of the beam, due for example to transverse thermal currents, gives a prediction for the system damping ratio.

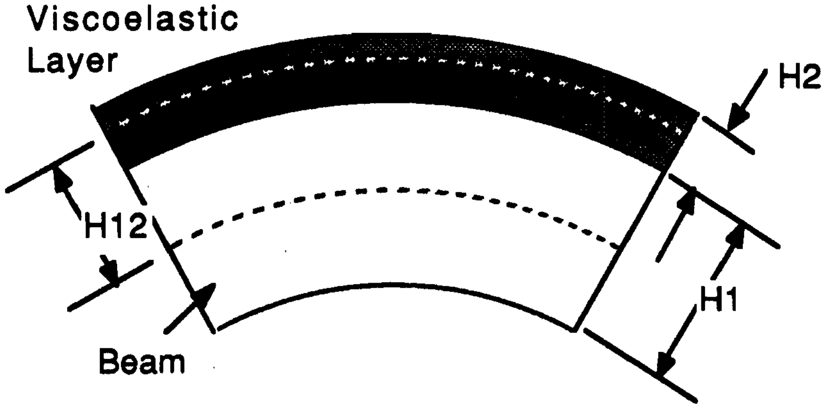

Figure1
Structure with free viscoelastic layer

When a constraining layer is added, shear effects must be included in the model (see Fig. 2.2). These effects depend on the curvature of the structure which can be seen in the governing equation (Kerwin, 1959),

$$\eta_1 = \eta' \frac{3E_3 t_3}{\pi E_1 t_1} \frac{\int_a^{a+L} \left[\frac{d^2 y}{dx^2}\right]^2 dx}{\int_0^l \left[\frac{d^2 y}{dx^2}\right]^2 dx} \tag{2}$$

where η_1 is the modified loss coefficient of a system, E_3 is the modulus of elasticity of the constraining layer, H_3 is the thickness of the layer, and η' is defined as the unmodified loss coefficient of a constrained structure given by,

$$\eta' = 4\pi \frac{1}{w} \left[\frac{\sinh(A)\sin(\theta/2) - \sin(B)\cos(\theta/2)}{\cosh(A) + \cos(B)} \right] \tag{3}$$

where,

$\tan^{-1}\theta = \beta_2$
$A = w\cos(\beta_2/2)$
$B = w\sin(\beta_2/2)$
$w = L_1/B_0$
$B_0 = (t_2 t_3 E_3/G_2)^{1/2}$
G_1=Shear modulus of viscoelastic material
t_i=Thickness of ith layer

Equations 2 and 3 show the dependance of the damping on the shearing of the viscoelastic layer, the bending of the base structure, and the length of the constraining layer.

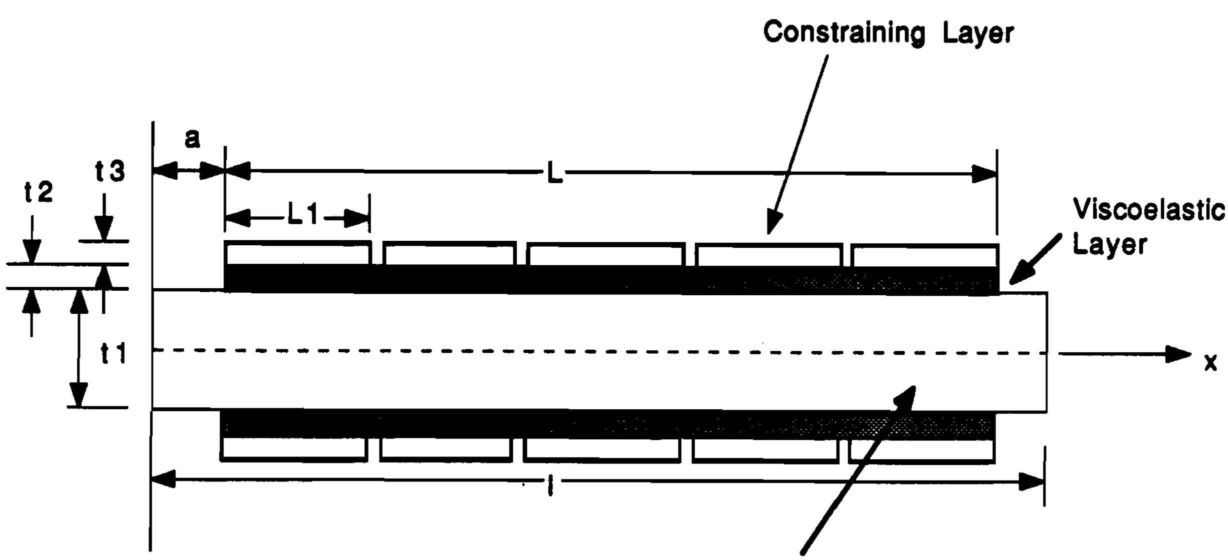

Figure 2
Segmented Constrained Beam

The relationship between the damping and the length of the constraining layer can be exploited to increase the loss factor. Most of the shearing of the viscoelastic layer occurs at the edges of the constraining layer. This effect can be seen in Figure 3. As a result, the number and length of the segments of the top layer can be optimized (Plunkett and Lee, 1970). One can further increase the loss of energy of a structure by extending the concept of viscoelastic damping by using multiple layers. There is another way to increase the damping however, by introducing non-linear damping.

Given the structure of a constrained viscoelastic damping layer, there are several ways one can introduce non-linear phenomena. One of these ways is to cause the segments of the constraining layer to impact (see Fig. 2.3). The impact would effectively add another energy dissipation mechanism. The only requirement is the careful spacing of the segments so they will touch. One drawback of this scheme is the difficulty of modeling the phenomena of impact damping.

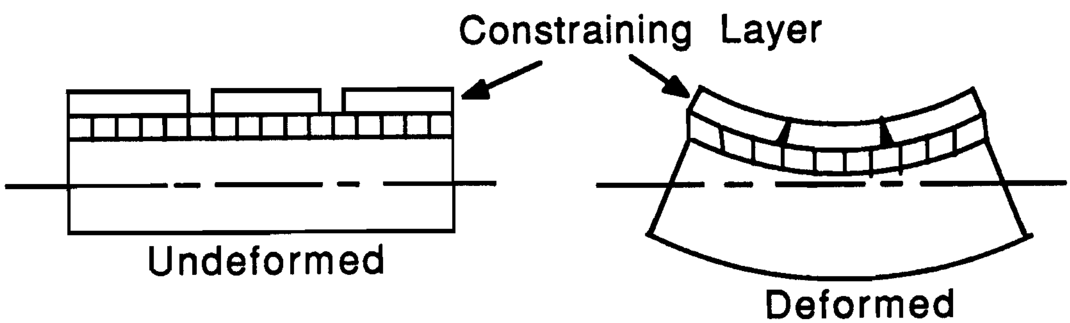

Figure 3
Non-linear damping mechanism

3 Experimental Apparatus

A set of experimental specimens was built to explore the possibility of added inpact damping. Six test specimens were constructed, each a beam (27" x 1" x 1/8") of 6061-T6 aluminum. Each beam was modified with a different damping mechanism, allowing the effect of each different layer to be observed separately. The first was a beam to determine the material damping without any damping treatment. Then a beam with a 1/16" thick free layer of Poron damping material on both faces was tested. An untreated area was left in the center for strain gauges. A third beam with a "continuous" constraining layer of 1/32" sheet aluminum was tested and compared to the unconstrained beam. In fact, the constraining layer was broken in the middle so that there were two segments. The length of the constraint segments was very close to the optimal length. Two beams tested were treated with segmented constraining layers which consisted of 10 2.625" segments on each side (see Fig. 4). One specimen had the segments separated by a small gap set by using a feeler gauge. This gap (.002") was chosen so that the segments would touch when the tip deflections of the free-free beam reached 1/2". The other beam had a gap of .01" - enough to guarantee separation. Finally, a beam with the same size segments bonded to the surface without a viscoelastic layer was tested. The segments were spaced so that they would touch when the tip deflection exceeded 1/2".

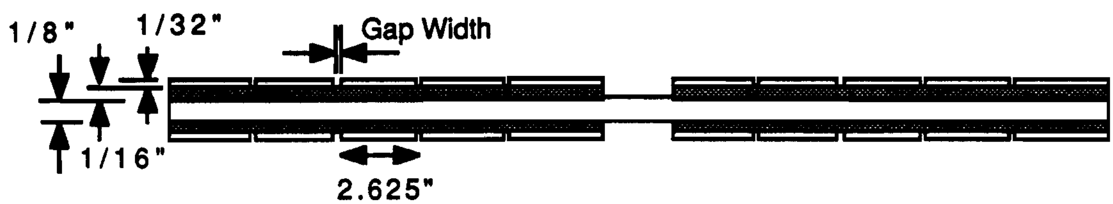

Figure 4
Test Specimen With Segmented Constrained Damping Layer

4. Experimental Procedure

Tests were performed in the ASTROVAC Space Simulation Facility at M.I.T. The ASTROVAC consists of a vacuum chamber (14' tall, 10' diameter), launcher, data acquisition system, and shaker system adapted for use in vacuum (see Fig. 5).

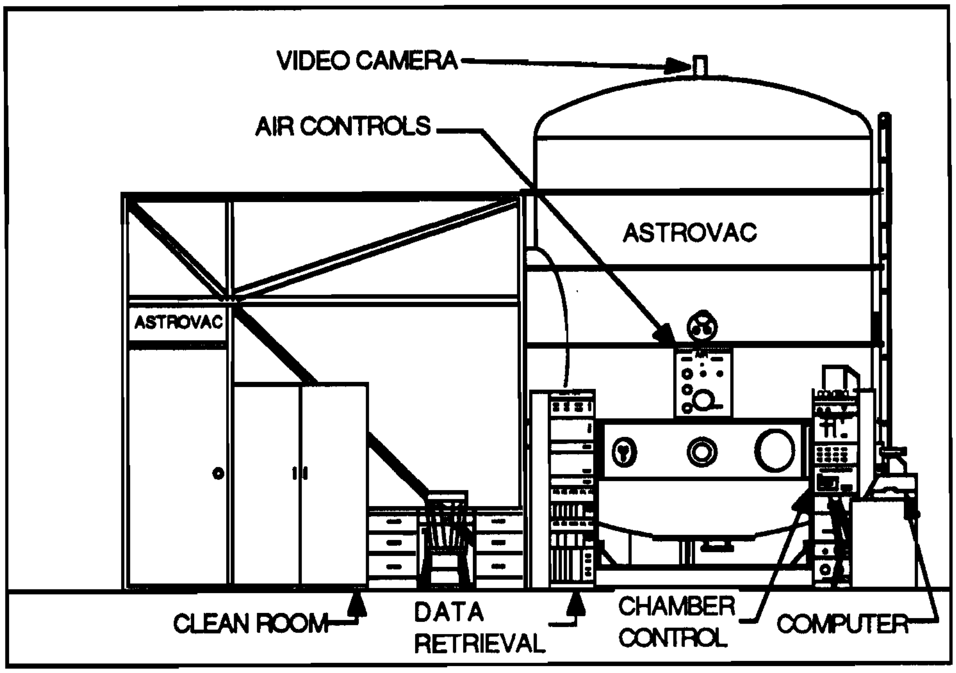

Figure 5
ASTROVAC Space Simulation Facility

Each test involved lofting a specimen in the ASTROVAC using the launcher (see Fig. 6). First, the specimen was set on the launch bed. Then the strain gauge wires were plugged into the follower which kept the short, light, leak wires slack during the test. Next, the vacuum chamber was evacuated to a pressure of 10^{-2} Torr and the beams were launched. While a beam was vibrating in free fall, the data from the strain gauges was sent to a CAMAC Crate for storage. Then the data was sent to an IBM XT for post-processing (Crawley, 1985).

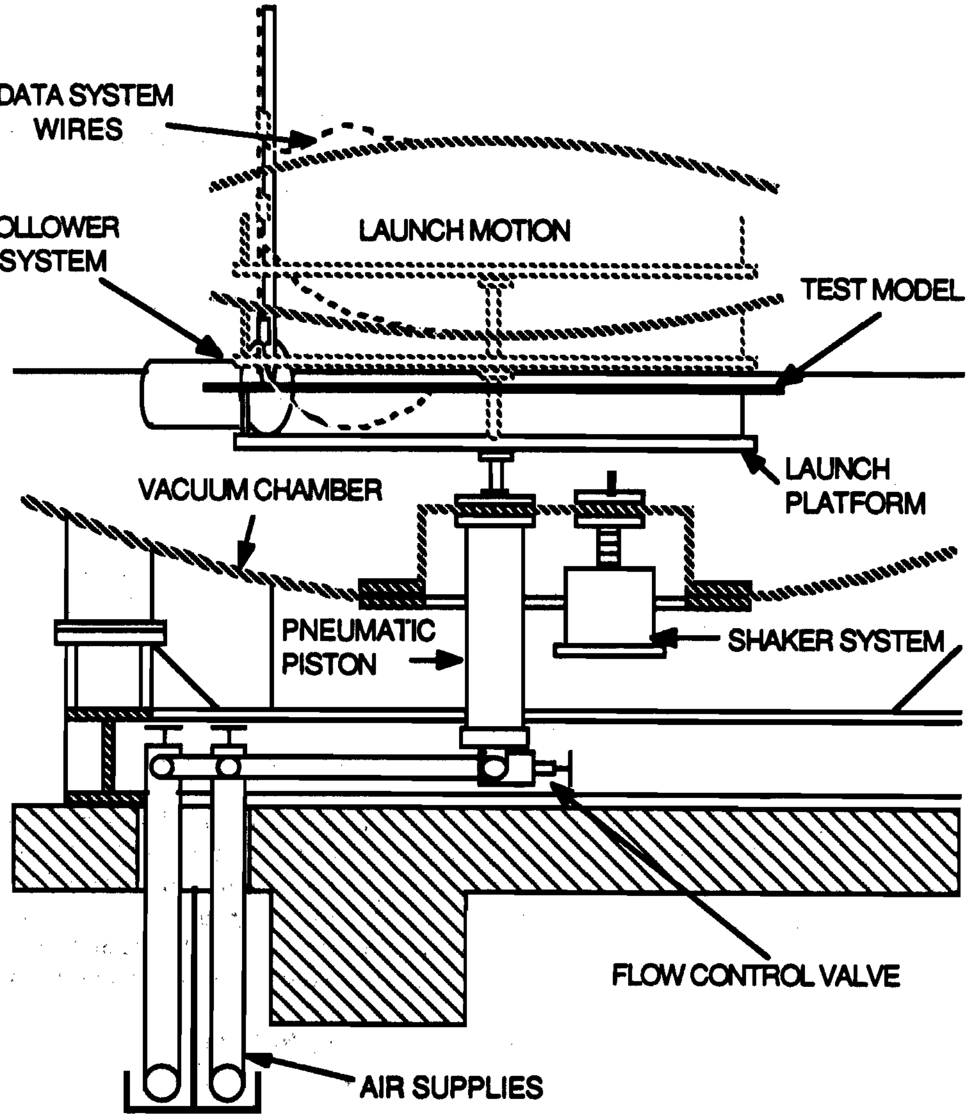

Figure 6
Launch of test specimen

5. Results

The strain data from each launch was plotted vs time (see Fig. 7). Damping ratios were obtained from plots using a log-decrement method.

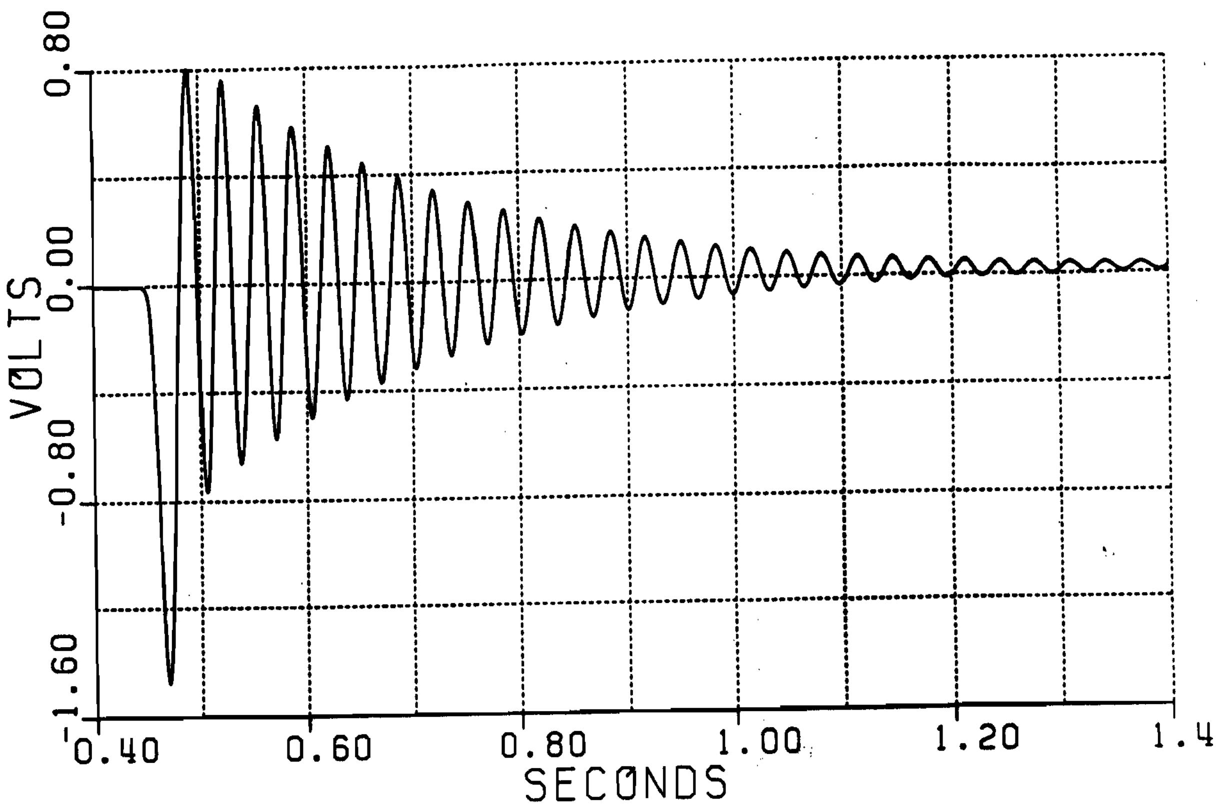

Figure 7
Sample plot of strain (volts) vs. time (seconds)

The damping ratios for each of the specimens is shown in Table 1 for an average of 6 launches. The beam with no damping layer showed the lowest damping while the beam with the segments of optimal length showed the largest damping increase. Comparing the results of the segmented constrained layer with linear and non-linear spacing, there was only a slight increase in damping. However, this increase was within the range of the scatter of the data. In addition, the damping ratio of the non-linear specimen showed little variation with amplitude.

Table 1 - Experimental Damping Results

Specimen	Damping Ratio, ζ (%)
Aluminum Beam	.08
Free damping layer	.10
2 segment constraining layer	3.99
10 segment constraining layer .002" gap width	1.97
10 segment constraining layer .01" gap width	2.15
10 segment bonded layer	.46

6. Conclusions

The comparison of experimental vs. theoretical results showed good correlation with theory (see Fig. 8). Damping ratio increase for the constrained segmented specimens, represented by CC and SCL (two element constraining layer, and 10 element constraining layer respectively) followed the pattern predicted by theory. The non-linear specimens represented by SCN and NNN (constrained damping layer and bonded layer with non-linear spacing respectively) showed little damping increase compared to their linear counterparts. This smaller than expected increase was probably due to several factors, the principle being manufacturing problems which made it difficult to accurately control the gap between the segments. Another possibility was that the plates did touch and the impact was too small to be significant.

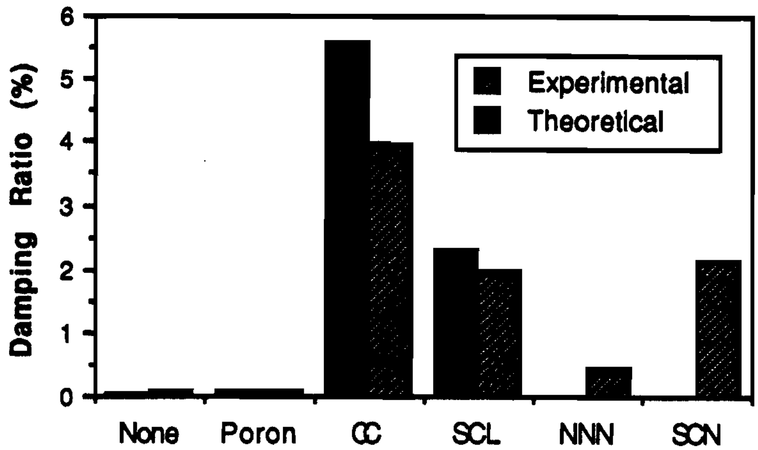

Figure 8
Experimental vs. theoretical damping ratios

References:

Kerwin, Edward M., 1959, "Damping of Flexural Waves by a Constrained Viscoelastic Layer," *The Journal of the Acoustical Society of America*, Vol. 31.

Crawley, E.F. and Mohr, D.G., 1985, "Experimental Measurements of Material Damping in Free Fall With Tunable Excitation," *AIAA Journal*, Vol. 23, No. 1, January 1985, pp. 125-131.

Plunkett, R. and Lee, C.T., 1970, "Length Optimization for Constrained Viscoelastic Layer Damping," *The Journal of the Acoustical Society of America*, Vol. 48.

Ungar, E.E., 1966, "Damping of Panels," *Noise and Vibration Control*, McGraw-Hill.